15th Triennial World Congress, Barcelona, Spain

A FEEDBACK INTERPRETATION OF VIBRATIONS IN HOT ROLLING MILLS

P. Belli [(*)], S. Bittanti [(∇)], M. Carandente [(∇)], A. De Marco [(∇)], S. Piana [(∇)]

[(*)] ABB Solutions, Via L. Lama 33, 20099 Sesto S.Giovanni (Mi),
[(∇)] Politecnico di Milano, Dip. di Elettronica e Informazione,
Piazza Leonardo da Vinci 32, 20133 Milano
Corresponding authors: bittanti@elet.polimi.it

Abstract: Hot rolling mills suffer of severe torsional vibration in particular working condition (thin thickness). These vibrations are often explained as the result of an exogenous disturbance amplified by a resonance effect. Herein, another interpretation is supported, namely the true origin is to be found in the interaction between the kinematic chain and the plastic deformation of the strip in the roll bite. Thus, the vibrations are the result of an unstable limit cycle due to these interacting dynamics. *Copyright © 2002 IFAC*

Keywords: steel industry, metals, torsional vibration, model, stability analysis

1 INTRODUCTION

The market of hot rolling mills has been characterised by an increasing demand in the production of strips with light gage thickness. This calls for an increased demand in the control performances; see (Nakagawa, et al. 1990; Grimble & Hearns 1999) for survey papers. In these mills, the kinematic chain may exhibit torsional oscillations during the strip-threading phase. For very thin strips, oscillations have non-negligible amplitudes and not fade out, causing loud noise and remarkable mass vibration of the stand. This phenomenon has been observed in many plants (Anbe et al. 1990; Doi, et al., 1987). Interestingly enough, such vibrations occur at the work rolls of the stands, whereas the main drive is not subject to vibrations. The neutralisation of this effect is a major task to guarantee the plant integrity. For, the basic preliminary task is to understand the origin of such vibration. This is the objective of this paper.
The paper is organised as follows: the models both of the kinematic chain and of the material in the roll bite is presented in section 2. By means of the overall system so obtained, it is possible to supply a sound explanation of the vibrations (section 3). Some typical experimental behaviours of the plant confirm our interpretation, as discussed in section 4.

2 THE MODEL

A Finishing Mill Stand (fig 1) consists of the kinematic chain, moved by the main drive, the stand with the hydraulic actuator and the material in the roll bite. In the figure and in the sequel, the acronym WR will be used for "work roll". A detailed description of the derivation of our model requires many pages, and is therefore omitted here due to limitations in space. Only the main steps of the derivation will be outlined.
As for the stand and the main drive, the models already available in the literature are used, and therefore their description is omitted for the sake of conciseness, see e.g. (Evans & Vaughan, 1996; Kugi, et al., 2001). The main focus is herein on the models of the kinematic chain and that of the material.

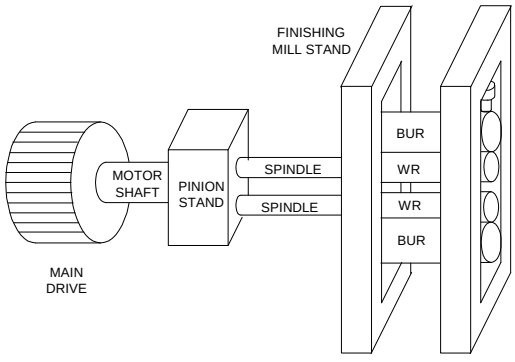

Fig. 1. Kinematic Chain - Typical Layout.

2.1 Kinematic chain model

The basic constitutive element of the kinematic chain is the torsional model of a shaft. Assuming the shaft homogeneous, it is possible to subdivide a shaft into a number of slices -say N- with a momentum of inertia $J_i=J_{shaft}/N$. Each slice is linked to the

surrounding slices with two springs, representing the torsional stiffness, see fig 2.

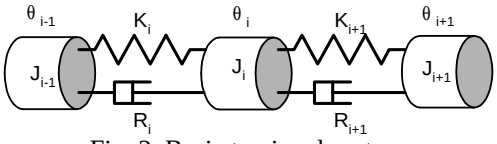

Fig. 2. Basic torsional system

The basic conservation equation for such a model is:

$$J_i\ddot{\vartheta} = -K_i\left(\vartheta_i - \vartheta_{i-1}\right) - K_{i+1}\left(\vartheta_i - \vartheta_{i+1}\right) + \\ - R_i\left(\dot{\vartheta}_i - \dot{\vartheta}_{i-1}\right) - R_{i+1}\left(\dot{\vartheta}_i - \dot{\vartheta}_{i+1}\right) + T_i \qquad (2.1)$$

where T_i is the external torque acting on the i-th slice. The same subdivision in slice has been applied to the full kinematic chain. Each device has been modelled using one, two or four inertias, as shown in fig. 3, where the blocks in dashed lines represent the main devices of the system. The equation 2.1 is replicated for the various inertias of the kinematic chain.

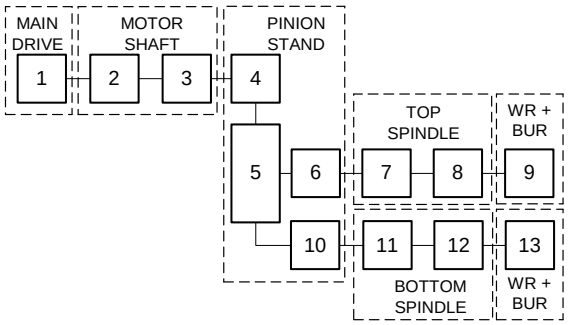

Fig. 3. Kinematic Chain Model.

Obviously, for specific parts of the chain, some terms of eq. 2.1 are missing. For instance, the extreme parts of the system, such as the main drive, require a single spring in their model.
In this way, modelling element by element the kinematic chain, the whole model worked out can be given the following compact matrix form:

$$\begin{bmatrix}\dot{\vartheta}\\ \ddot{\vartheta}\end{bmatrix} = \mathbf{A}\begin{bmatrix}\vartheta\\ \dot{\vartheta}\end{bmatrix} + \mathbf{B}\begin{bmatrix}T_M\\ T_R^T\\ T_R^B\end{bmatrix}; \qquad \begin{bmatrix}\omega_M\\ \omega_{WR}^T\\ \omega_{WR}^B\end{bmatrix} = \mathbf{C}\begin{bmatrix}\vartheta\\ \dot{\vartheta}\end{bmatrix} \qquad (2.2)$$

Where the state variables are angular displacements organised in the vector ϑ and the angular speed (vector $\dot{\vartheta}$) of each inertia; the inputs are the main drive torque (T_M), top WR resistant torque (T_R^T) and bottom WR resistant torque (T_R^B); the outputs are the main drive speed (ω_M), top and bottom WR angular speed (ω_{WR}^T , ω_{WR}^B); **A**, **B** and **C** are 3 matrices describing dynamic behaviour of the system.

2.2 Modelling the plastic deformation process

The WR resistant torques (T_R^T and T_R^B for the top and bottom rolls, respectively) act as inputs for the kinematic chain. In many papers they are taken as exogenous signals, see e.g. (Anbe et al., 1990; Doi, et al., 1987). Herein, the resistant torque is considered as a dynamic function of the plastic deformation of the material in the roll bite. Precisely, the resistant torques on the WRs is assumed to be depend upon i) the force F_R actuated by the stand on the strip and ii) the WR speeds ω_{WR}^B (bottom) and ω_{WR}^T (top). Thus, the conceptual block-diagram of the whole system is depicted in fig. 4, where h_2 denotes the strip thickness at the exit of the roll bite.

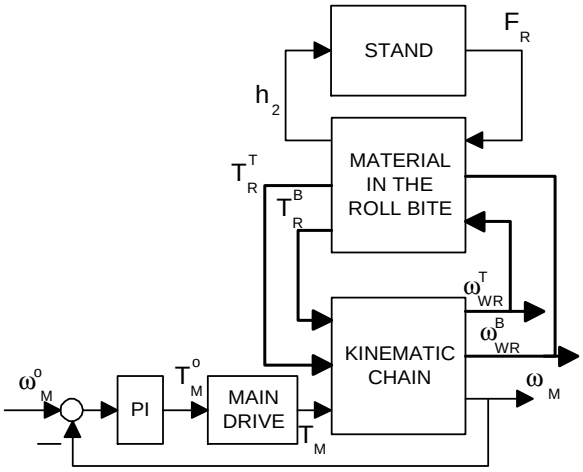

Fig. 4. Interaction between Kinematic chain and strip

The purpose of this Section is the development of the mathematical model of the material in the roll bite behaviour. The existing literature on this process enumerates a number of publications devoted to static models (Orowan, 1943; Tselikov, 1967), from which design correlations, describing the relevant variables (rolling force and torque, speed, thickness, etc), have been developed. The dynamic model here proposed takes advantage of these studies, but it also considers dynamic phenomena related to the mass storage of material in the roll bite and to the stick-slipping dynamic behaviour. With the model here presented, it is possible to explain the occurrence of vibrations.

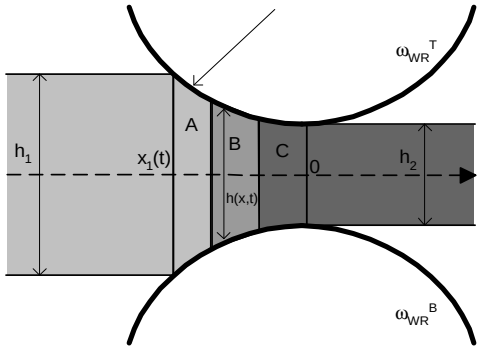

Fig. 5. Slip-sticking friction in the roll bite.

With reference to fig. 5, the main assumptions carried out are:

- The rolling pressure is constant in the entire contact area.

- The neutral point (i.e. the point where the average velocity of the strip coincide with the WR velocity) is placed at the exit of roll bite, so that $u_2 = \omega_{WR}^M R_{WR}$, where ω_{WR}^M is the average of WR speed.
- WRs are undeformable.

The strip model is developed in two steps, by writing first the mass conservation equations and then passing to the description of the stick-slipping behaviour.

Mass conservation. With h(t,x) and u(t,x) are denoted the thickness and the average speed of the strip at time t and longitudinal coordinate x. Following the lead of Pawelski, et al. (1987), the one-dimensional mass conservation equation is easily derived as:

$$\frac{\partial h}{\partial t} + \frac{\partial (u\, h)}{\partial x} = 0 \qquad (2.3)$$

The conservation equation (2.3) has been integrated along the arc of contact. For the integration of first term, it has been taken into account that: the lower integration limit depends on time and the arc of contact can be assumed to be parabolic. For the integration of second terms has been taken into account the steady state mass conservation equation ($h_1u_1=h_2u_2$) and the strip reduction (h_1-h_2) has been calculated inverting the following well-known formula (Ginzburg, 1989):

$$F_R = \sigma\left(\omega_{WR}^M\right)\sqrt{R_{WR}\left(h_1 - h_2\right)} \qquad (2.4)$$

The result is:

$$\sqrt{R_{WR}\left(h_1 - h_2\right)}\,\dot{h}_2 = -\omega_{WR}^M R_{WR} h_2 + \ldots$$
$$\ldots + h_1 \omega_{WR}^M \left(R_{WR} - \frac{F_R^2}{h_1\, \sigma^2\left(\omega_{WR}^M\right)} \right) \qquad (2.5)$$

A linearized version of this equation is obtained as:

$$\tau\, \delta \dot{h}_2^* + \delta h_2^* + \frac{h_{20}}{h_{10} - h_{20}} (1-\alpha) \delta\omega_{WR}^* + 2\delta F_R^* = 0 \qquad (2.6)$$

Where the subscript 0 is used to indicate evaluation of the variable at the steady state; as usual, δ denote variation; and finally the following assumption has been carried out:

$$\delta h_2^* = \frac{\delta h_2}{h_{10} - h_{20}} \quad \delta\omega_{WR}^* = \frac{\delta\omega_{WR}^M}{\omega_{WR0}} \quad \delta F_R^* = \frac{\delta F_R}{F_{R0}}$$

$$\tau = \frac{1}{\omega_{WR0}} \sqrt{\frac{(h_{10} - h_{20})}{R_{WR}}} \qquad \alpha = \frac{1}{R_{WR}} \frac{h_{10}}{h_{20}} \frac{\partial u_1}{\partial \omega_{WR}}\bigg|_0$$

In the sequel, this linearized equation will be used, which suffices to obtain a fair description around the steady-state. In particular, it enables the study of the stability of the kinematic-material loop.

Stick-slipping behaviour. As shown in fig. 4, rolling torques are the exit signals of material model towards the kinematic chain model. In order to calculate the rolling torque, it is necessary to investigate in depth the interaction between the roll surface and the rolled material see e.g. (Orowan, 1943).

Herein, a dynamical modelization of such interaction will be presented. Precisely, the contact takes place through two surfaces, the upper contact surface and the lower one.

Moreover, various types of contact areas will be distinguished, since in some points the material is stuck to the WR surface, whereas in other points slipping takes place. Precisely, three different areas of contact between the material and the WR surfaces are considered (see fig. 5). Only in the intermediate area B, sticking occurs, while, in the remaining parts, the slipping effect dominates. Correspondingly, the friction coefficient is the static coefficient μ_S in area B and the dynamic coefficient μ_d in the other parts, with $\mu_D < \mu_S$. Actually, having assumed that the neutral point is practically located at the exit of the roll bite, the area C may be neglected. In conclusion, the torque generated in an elementary contact area ΔS is given by $\Delta T_R = \mu_i\, p_R\, \Delta S\, R_{WR}$, where $\mu_i = \mu_S$ in the zone B, and $\mu_i = \mu_D$ other-where. By integrating over the whole contact area, one can define the resultant friction coefficient as $\mu_S\, f_u + \mu_D\left(1 - f_u\right)$. The coefficient f_u appearing here is the ratio between the area of zone B and the total area of contact. In other words, it is the sticking fraction. Obviously $f_u \in [0,1]$, but, as a matter of fact, the sticking fraction ranges, in steady state conditions, in a narrower interval, say $f_u \in [f_1, f_2]$ due to physical constraints, depending mainly on the state of the strip surface. It has been assumed that these limits are the upper and lower bounds also in transient conditions.

Considering that the vertical force is given by eq. (2.4), the torque acting on the top contact surface is given by:

$$T_R^T = \sigma\sqrt{R_{WR}\left(h_1 - h_2\right)}\, R_{WR} \left(\mu_S\, f_u^T + \mu_D\left(1 - f_u^T\right)\right) \qquad (2.7)$$

Actually, this is the top WR torque: an entirely analogous equation holds for the bottom WR, torque. Obviously, f_u^T denotes the sticking fraction for the upper WR; f_u^B will denote the same fraction for the bottom WR.

Notice that the partition of the contact area in sub-areas with different friction coefficients is made in many papers, as in (Ekelund, 1933; Ginzburg, 1989). The main innovative contribution of this paper is to consider the possibility of a time variability in the sticking fractions f_u^T and f_u^B. Indeed, against a sudden increment in the WR speed, the equilibrium between the sticking and slip breaks down, and the stick zone (zone B) undergoes a sudden shrinkage;

after some time, this effect fades out. Correspondingly, after a sudden reduction of coefficient f_u^T, there is a transient, at the end of which, f_u^T recovers the initial value. The following dynamic relation captures this:

$$\delta f_u^{*T} = -\frac{s\, k_d\, \tau_d}{1+s\,\tau_d}\,\delta\omega_{WR}^{*\ T} \qquad (2.8)$$

where, k_d and τ_d are parameters dependent on physical variables (temperature, material characteristic etc.) and:

$$\delta f_u^{*T} = \frac{f_u^T - f_{u0}^T}{f_{u0}^T}\ . \qquad \delta\omega_{WR}^{*\ T} = \frac{\omega_{WR}^T - \omega_{WR0}^T}{\omega_{WR0}^T}$$

Remark (the non-minimum phase behaviour)
The qualitative behaviour of the torque can be easily worked out on the basis of the previous considerations. Precisely, the transfer function from the WR speed to the top rolling torque T_R^T (obtained from the above equations by linearizing the output transformation) is given by:

$$\frac{\delta T_R^{*T}}{\delta\omega_{WR}^{*\ T}} = -\frac{k_h\left[\tau\tau_d\frac{k_f}{k_h}s^2 + \tau_d\left(\frac{k_f}{k_h}-1\right)s - 1\right]}{(\tau s+1)(\tau_d s+1)} \qquad (2.9)$$

and analogously for the bottom rolling torque δT_u^{*B}. Note that such function has always a non-minimum phase zero.

3. THE VIBRATION ENIGMA EXPLAINED

The overall block diagram is depicted in Fig. 6, where Z_{ij} are the kinematic chain transfer function, A(s) is the transfer function of the main drive, "MATERIAL MODEL" is the non-linear model of plastic deformation in the roll bite.

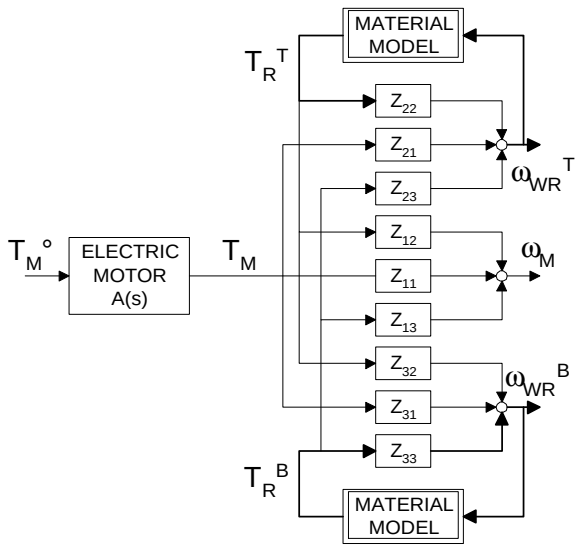

Fig. 6. Process block diagram.

As can be seen, there are two feedback loops, for the top and bottom WR's. Second, all system blocks are linear with the exception of the models of the top and bottom plastic deformation. Precisely, in these two non-linear blocks, the nonlinearity comes from the structure of the equation of the rolling torques (eq. 2.7). Besides that, there is another fundamental nonlinearity, namely the upper and lower bounds f_1, and f_2 for the sticking fractions f_u^T and f_u^B.

The plant is operated in closed-loop as indicated in fig. 4. The speed control block is simply a proportional-integral controller. Note that the main drive is equipped with a motor torque regulator. The behaviour of these blocks closing the loop is known.

A Simulink-based simulator of the rolling process has been developed. The parameters of the model are the mechanical data (inertia's, stiffness, geometrical dimensions, etc.) and the steady state conditions (rolling schedule, friction coefficients, yield stress, etc.). In this paper, as steady state conditions have been considered those associated with a low thickness strip production (between 1.5 and 2 mm).

Each loop in Fig. 6 can be diagrammatically sketched as indicated in Fig. 7, which makes reference to the top WR. Note that $Z_{22}(s)$ is the transfer function expressing the effect of the rolling torque on the WR speed and F(s) is the transfer functions of the linearized model relating the WR speed to the rolling torque (eq. 2.9). Such simple scheme has the feature of pointing out the interaction between the material plastic deformation effect and the process kinematics.

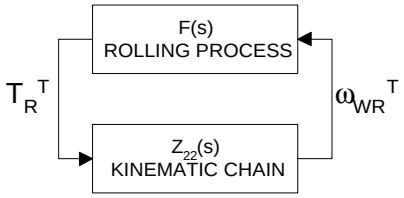

Fig. 7. The Basic Feedback Loop.

The Bode diagrams of the obtained open-loop transfer function $L(s)=F(s)Z_{22}(s)$ is shown in Fig. 8. From these diagrams, it turns out that the elementary feedback loop is unstable, note that at approx. 100 rad/s the gain is grater than 0 dB and the phase delay is greater than 180°.

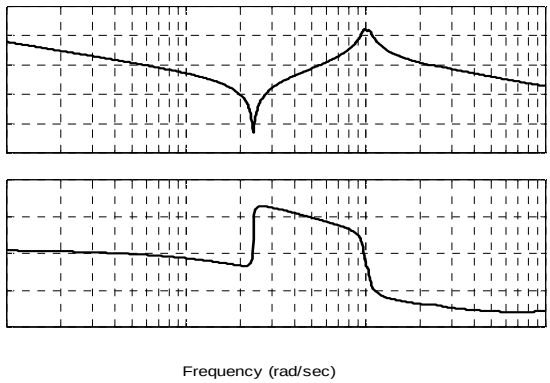

Fig. 8. Open Loop Bode Diagram.

Passing now to the overall system of fig. 6, the model

can be linearized by replacing the non-linear blocks representing the plastic deformation of the material in the roll bite with the transfer function F(s).

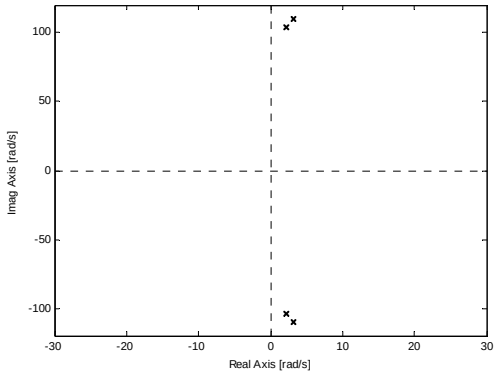

Fig. 9. Closed Loop Pole Map.

Fig. 9 shows low frequency system poles, when the two loops created by function F(s) are closed. It is important to note that there are two pairs of unstable and complex conjugate eigenvalues. The imaginary parts of the unstable eigenvalues are slightly different, 16.5 Hz (104 rad/s) for a pair and 17.5 Hz (110 rad/s) for the other.

This closed loop instability means that the equilibrium point corresponding to the considered working conditions is not attractive. Consequently, the overall plant cannot keep a steady-state working condition; rather, the variables evolve towards a limit cycle, whose characteristics are imposed by the specific non-linearity of the plant. In this way, it is possible to explain the oscillatory behaviour experimentally observed in hot rolling mills during the production of low thickness (less than 2 mm.) strips.

Usually, the oscillations observed in hot rolling mills are explained as a resonance effect activated by an external periodic disturbance, e.g. a torque ripple generated by the cyclo-converters. Herein, an innovative viewpoint is provided, consisting in viewing the vibrations as a by-product of instability of the equilibrium point in a feedback loop. Instability arises due to the interaction of the inherent resonance of the kinematic chain with the dynamical behaviour of the material deformation in the roll bite. Usually, the rolling torque is seen as a constant. Alternatively, the dependence of the torque upon the working roll speed is described by an algebraic relation (Wang 1998). Here, a proper modelization is investigated, where the dynamical behaviour of the material deformation in the roll bite is duly considered. Eventually, this leads to explain vibrations as an instability effect of a feedback system.

4 IS THE FEEDBACK INTERPRETATION OF VIBRATIONS SUPPORTED BY THE EXPERIMENTAL EVIDENCE?

Above has been presented a model explaining the vibrations in terms of feedback instability in the loop generated by the interaction of the kinematics with the material deformation. However, as in any scientific investigation, the only way of substantiating a theory is to look for its experimental evidence.

The main process variables have been measured, Precisely, measurements refer to the stand where vibrations were observed (typically this is the second or third stand out of six stands). Among plus of 100 signals measured, it is important to quote the top and bottom WR speeds (taken with laser device) and torsional torque through the spindles (by means of two strain gauges installed on each spindles close to the WR). However, the determination of the rolling torque appearing in our model requires a computation based on the kinematic chain equation.

The measurements have been repeated in various work conditions, for final thickness (at the exit of the last stand) ranging from 1.5 mm to 5 mm. These following diagrams refer to measurements in stand 3 of a hot strip mill plant with 6 stands, where the final thickness was 1.8 mm and vibrations were observed.

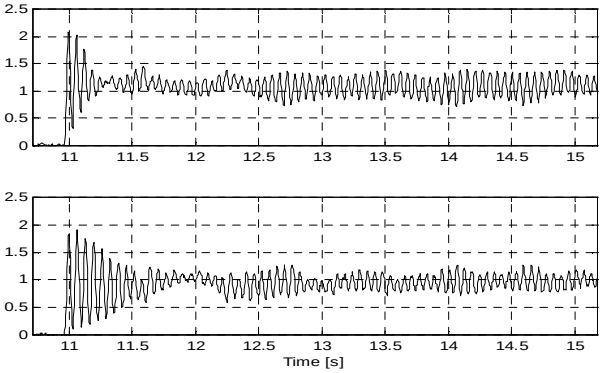

Fig. 10. Torque measured on the spindles.

As can be seen in Fig. 10, there is an initial phase (the so-called threading phase) during which the high intensity vibrations occur, followed by a damping phase. In normal conditions (thickness above 2 mm.), the damping is effective, and vibrations fade out. On the opposite, in our case, after the initial transient, there is a permanent oscillation on both top and bottom shafts. The frequency of the oscillations is about 17 Hz. Furthermore, the two oscillations are out of phase (the max-peak of the top spindle corresponds to a min-peak for the bottom spindle).

4.1 The traditional explanation

The usual way of explaining the vibrational effects is that vibrations are the result of exogenous disturbances acting on the kinematic chain. The candidate disturbance is the motor torque ripple produced by the cyclo-converter, amplified by the chain resonance effect. According to this interpretation, oscillations are explained by means of the kinematic chain only, as a purely mechanical resonance effect.

To probe this possible explanation, the spectrum of the electric motor torque has been compared with the

spectrum of the torque through the spindle (both signals are measured). If the usual explanation were correct, the peak of the two spectra should coincide each other, and should coincide with the resonance frequency of the chain (frequency which can be easily computed and turns out to be 16.5 Hz). Actually, the analysis of the two spectra does not support the above expectation: There is no apparent correlation between the signals.
A second clue against this explanation is a typical feature of the top and bottom signals: once the threading transient has been fade out, they are out of phase, as can be seen from fig. 10. This feature was observed in all measurement trials, and is well known to the field specialists. Suppose again that the vibrations were produced by an exogenous signal; since the pinion stand produces an equal subdivision of the motor torque, and the transmission chains along the two shafts are almost coincident, the motor acts in the same manner on the two WR. Therefore the top and bottom oscillations should be in phase.

4.2 Feedback explains vibrations

In fig. 11, it is reported a simulation performed with our model referring to the same rolling conditions of those associated with the experimental data of fig.10.

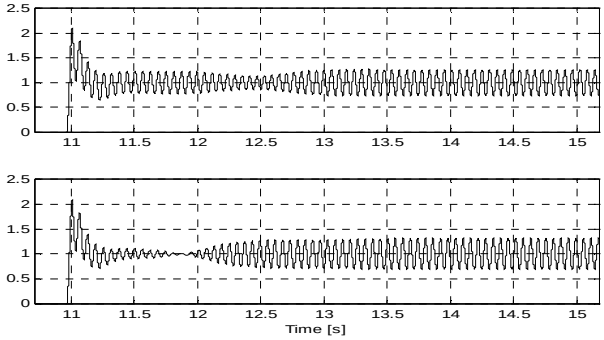

Fig. 11. Simulation results of torque through the spindles.

The comparison of the simulated trial and the real data is convincing evidence in favour of the validity of the model. Again fig. 11 shows that during the threading phase the rolling torque vibrations in the top and bottom WR are in phase; then, after a period of apparent fading, they turn to become persistent in time, and out of phase.

5. CONCLUDING REMARKS

In this paper, an explanation on the phenomenon of vibrations in hot rolling mills is provided. Usually, vibrations are interpreted in terms of resonance effects triggered by torque ripples due to cyclo-converters. By analysing experimental data, it is shown that this interpretation is not sound, and instead an explanation in terms of instability in closed loop is proposed.

ACKNOWLEDGEMENT

Paper supported by the National Research Project "New Techniques for the Identification and Adaptive Control of Industrial Systems". Part of the activity leading to this paper was developed during the stage of M. Carandente and S. Piana, former students of the Politecnico di Milano, at Danieli Wean United under the supervision of P. Belli.

REFERENCE

Anbe Y., D.H.E. Butler, M.A. Churches, E.R. Vergan, (1990). Compensation of a Digitally Controlled Static Power Converter for a Damping of Rolling Mill Torsional Vibration. *IEEE Transaction on Industry Applications Society*

Doi K. etc. (1987), Analysis and Control Systems for Shaft Vibration in Steel Rolling Processes. *Kawasaki Steel Giho*

Ekelund S. (1933). Analysis of Factors Influencing Rolling Pressure and Power Consumption in the Hot Rolling of Steel. *Steel* **93**.

Evans P. R., N. D. Vaughan (1996). Dynamic characterisation of a rolling mill. *Journal of System and Control Engineering*, **210** pp. 259÷271

Ginzburg V. B. (1989). In: *Steel–Rolling Technology – Theory and practice*. Marcel Dekker Inc., New York

Grimble, M.J., G. Hearns (1999). Advanced Control for Hot Rolling Mills. *Advance Control*, Highlights of ECC'99 (P.M. Frank ed.), Springer, London, pp.135-169.

Kugi A., R. Novak, K. Schlacher (2001). Non-linear Control in Rolling Mills: A new Perspective. *IEEE Transaction on Industry Applications*.

Nakagawa S., Miura H., Fukushima S. & Amasaki J. (1990). Gauge Control System for Hot Strip Finishing Mill. *29th Conference on Decision and Control*, Honolulu, USA, pp. 1573-1578.

Orowan E. (1943), The calculation of Roll Pressure in Hot and Cold Flat Rolling. *Proc. Institute of Mechanical Engineers*, Vol. 150, pp. 140-167

Pawelski O., W. Rasp, K. Friedewald (1987). Chatter in cold Rolling. Theory of interaction of plastic and elastic deformations. *Proc. Of the 4th International Steel Rolling Conference*, Vol. 2 pag. E11.1÷E11.5

Tselicov A. (1967), In: *STRESS and STRAIN in METAL ROLLING*. MIR Publishers, Moscow

Wang Z., D. Wang (1998), Method of judging the self-excited vibration of rolling main drive system in rolling slippage, *Journal of Sound and Vibration* **215(5)**, pp. 1135-1143